First-principles study of the electronic and magnetic structure of $c(2\times2)$ sulfur chemisorbed above Fe(001)

S. R. Chubb and W. E. Pickett
Condensed Matter Physics Branch, Condensed Matter and Radiation Science Division, Naval Research Laboratory, Washington, D.C. 20375-5000
(Received 9 February 1988)

We have performed the first, first-principles study of the adsorption of sulfur above a magnetic, Fe surface. Our results, derived from the all-electron, film full-potential linearized augmented-plane-wave method applied to a seven-layer Fe film with and without $c(2\times2)$ layers of S positioned next to the two surface Fe [Fe(*S*)] layers, include determinations of the equilibrium sulfur height (H_{eq}) and vibrational frequency, as well as the associated electronic and magnetic structures. We find excellent agreement between our calculated value (1.12 Å) of H_{eq} with the earlier result [1.09(5) Å] derived by Legg, Jona, Jepsen, and Marcus from a dynamical low-energy electron diffraction intensity analysis. The adsorption induces antibonding minority surface states immediately above and below E_F which play an important role both in reducing the magnetic moment of the Fe(*S*) atom (by $\sim20\%$) and in the rather small calculated increase (0.85 eV) in work function. These states should be clearly resolvable in both integrated and angle-resolved, spin-polarized photoemission and inverse-photoemission experiments. We present additional predictions, including the adsorption-induced changes in the hyperfine fields and in the angle-resolved, spin-polarized surface state spectra, and relate our findings to questions associated with the sulfur-induced poisoning of an iron catalyst.

I. INTRODUCTION

Although it is well known that the catalytic value of iron in various processes is readily poisoned by introduction of small amounts of a sulfur contaminant, not only is surprisingly little known about the origins of this poisoning effect, very little is known at the microscopic level about the interaction of sulfur with iron. The impact of sulfur contamination on the magnetic properties of iron is even less well understood.

For a variety of reasons, the chemisorption of S on Fe provides a natural setting in which the factors responsible for the sulfur-induced poisoning of an Fe catalyst can be isolated. Specifically, with modern ultrahigh-vacuum procedures, precise, reproducible results for the surface geometry of a specific chemisorption can be derived under controlled conditions using probes of the surface region such as low-energy electron diffraction (LEED), surface extended x-ray absorption fine-structure spectroscopy (SEXAFS), and near-edge x-ray absorption fine-structure spectroscopy (NEXAFS). In turn, non-spin-polarized and spin-polarized ultraviolet photoemission spectrum (UPS) and angle-resolved photoemission spectrum (ARUPS), x-ray photoemission spectrum (XPS), and inverse photoemission spectrum (IPS) and k-resolved inverse photoemission spectrum (KRIPES) measurements, made within this controlled setting, provide detailed information about the electronic and magnetic structures of surfaces. Complementing these experimental probes are theoretical tools [such as the all-electron full-potential linearized augmented-plane-wave method[1,2] (FLAPW)] for determining from first-principles the geometry and electronic and magnetic structures of surfaces and the associated adsorption-induced changes which result from chemisorptions.

Additional incentive for understanding the chemisorption of S on Fe theoretically and experimentally is provided by (1) the lack of detailed information concerning gaseous chemisorptions on Fe surfaces, (2) the need to test both the theoretical and experimental probes of surface electronic and magnetic structure with a material which is strongly magnetic, and (3) the need to better understand the interplay between magnetism and electronic structure in chemisorptions on magnetic surfaces. More specifically, though various experimental studies have been made of gaseous chemisorptions on Fe surfaces, only the chemisorption of O on Fe(001) has been studied theoretically with spin-polarized, self-consistent methods, in which both the geometry and electronic and magnetic structures have been determined from first principles.[3] Only a handful of such fully *ab initio* studies of gaseous chemisorptions have been made,[3-5] on any transition-metal surface, and only two of these involved magnetic surfaces [Fe(001) (Ref. 3) and Ni(001) (Ref. 4)].

Of the various possible chemisorptions of S on Fe surfaces, the case of S adsorbed on Fe(001) has been most widely studied and is best characterized. Ueda and Shimizu[6] first observed a centered 2×2 [$c(2\times2)$] (Ref. 7) LEED pattern during a series of work-function measurements at different coverages of S. They concluded that the iron work function shifted continuously from 4.67(3) eV at zero coverage to $\sim5.21(3)$ eV at the $c(2\times2)$ coverage. Later, Legg, Jona, Jepsen, and Marcus[8] (henceforth, LJJM) also determined from LEED and Auger electron spectroscopy measurements that S chemisorbs in an ordered $c(2\times2)$ overlayer and from a dynamical LEED intensity analysis inferred that the S is located 1.09(5) Å above the fourfold hollow. At greater coverages, LJJM

 ©1988 The American Physical Society

observed the "growth of an amorphous sulfur film." DiDio, Plummer, and Graham[9] (DPG) performed non-spin-polarized angle-resolved photoemission experiments in which they identified the adsorbate-induced bands which accompany this $c(2\times2)$ S/Fe(001) chemisorption. Fernando and Wilkins[10] (henceforth, FW) carried out non-spin-polarized LAPW calculations using the geometry proposed by LJJM but did not find very good agreement with the results of either Ueda and Shimizu[6] or DPG.[9] Nonetheless, these authors made various inferences concerning the reasons for sulfur poisoning. To date there have been no published measurements of the ironlike spectrum after the adsorption, nor is there information concerning the magnetic effects associated with $c(2\times2)$ S/Fe(001). The importance of magnetic ordering in the poisoning by S is also unexplored.

In this paper, we present various results from the first *ab initio* study of this chemisorption, in which the impact of magnetic order on electronic structure is included and the height of the adsorbate is determined from first principles. This is also the first study of S chemisorbed above any Fe surface to incorporate the effects of magnetism. Our motivation has been to examine the effects of magnetism on the adsorption process, to compare with our previous studies of $p(1\times1)$ O chemisorbed on Fe(001), and if possible to gain insight into the poisoning phenomenon through a detailed analysis of the adsorption-induced modifications of electronic and magnetic structure. The paper includes a review of the associated changes in the spatial distributions of charge from both the occupied and unoccupied portions of the spectrum, an examination of the adsorption-induced changes in the surface magnetism and spin-resolved densities of states (DOS's) and spin- and k-resolved band structures. In the course of the analysis, we have found a number of important differences between our results and those derived by FW which have indirect bearing on understanding the S-induced poisoning of an Fe catalyst. Because their LAPW calculations are similar to ours except that they did not include the effects of magnetism in their work, we have inferred that magnetic ordering has an impact on the poisoning of iron surfaces. Also, through the analysis, we have learned that the impact of various adsorption-induced changes in electronic structure associated with the chemisorption have been ignored in earlier analyses of photoemission data and may have bearing on the poisoning phenomenon.

We begin in the next section by examining our method of calculation. In Sec. III we present the results of our first-principles determinations of the adsorbate height (H_{eq}) (which we find to be in excellent agreement with the height inferred by LJJM) and perpendicular frequency. Here, we also discuss our calculated change in work function ($\Delta\Phi_{eq}$) at H_{eq}, the dependence of $\Delta\Phi$ on changes in the height, and the underlying modifications of electronic structure which lead to the rather small increase in our calculated value of $\Delta\Phi_{eq}$. Because our calculated value for $\Delta\Phi_{eq}$ is in considerably better agreement than the value found by FW with experiment, we also contrast various differences between the adsorption-induced changes in charge which were found in the two calculations and which are responsible for the different values of $\Delta\Phi_{eq}$.

In Sec. IV we turn to an analysis of our calculated densities of states and the associated adsorption-induced modifications of the eigenvalue spectrum. We also present various spin- and energy-resolved density plots which help us to identify the nature of the bonding and the character of the sulfur-induced modifications of the Fe spectrum. These plots reveal that the presence of the sulfur is responsible for important modifications of the d bonding both in the surface Fe [Fe(S)] and first subsurface Fe [Fe($S-1$)] layers as a consequence of the adsorption.

We present in Sec. V a discussion of the k-resolved band structures, where we make various comparisons with the results of DPG (Ref. 9) and provide detailed information concerning the adsorption-induced modifications of the Fe surface states (SS's) and surface resonance (SR) states. Through this analysis and information from the previous section, we are able to identify various new features, especially in the minority state spectrum, which not only should be clearly resolvable in spin-resolved UPS, ARUPS, IPS, and KRIPES measurements but have bearing on the poisoning of Fe catalysis by sulfur. In addition, we infer from the existence of these changes (which lead to a considerably smaller charge transfer to the sulfur than was found by FW (Ref. 10) and are responsible for the better agreement that we find with experiment for the change in work function[6]) that the interplay between magnetic ordering and electronic structure has an impact on the poisoning. In the sixth section, we present results for the adsorption-induced changes in various magnetic quantities. Experimental verification of these findings would provide an additional, important check of the accuracy of our results.

In the final section, we examine the implications of our findings on the question of sulfur-induced poisoning. Here, we infer from our calculated changes in the DOS's and band structures, as well as from spatially resolved difference plots of unoccupied portions of the spectrum that the underlying physics of the poisoning phenomenon is due to a reduction in the minority DOS near the Fermi energy and a shift of unoccupied states away from the region near the Fe surface, rather than due to a large electrostatic shift of the Fermi level as was suggested by FW previously.[10]

II. METHOD

We have determined the equilibrium binding of $c(2\times2)$ S/Fe(001) using the full-potential, linearized, augmented-plane-wave method developed by Wimmer *et al.*[1] and Weinert *et al.*[2] for thin films, which provides not only accurate magnetic and electronic structures but a precise determination of the electrostatic energy. Because this method incorporates the correct boundary conditions and electrostatics in the vacuum regions above and below the outer layers of the film, it provides accurate values for the work function.

In the current study, we used the exchange-correlation potential due to von Barth and Hedin.[11] We performed

our calculations using a seven-layer Fe slab with and without an additional $c(2\times2)$ S layer positioned next to the two outer Fe surface layers. The S is placed in the fourfold hollow as suggested by LJJM. The equilibrium height H_{eq} and perpendicular vibrational frequency are determined from a parabolic fit to the total energies derived from fully self-consistent calculations, carried out for each of the three heights: 1.05, 1.09, and 1.14 Å. Because in the presence of the adsorbate, each layer of the film requires two Fe atoms [since the $c(2\times2)$ layer corresponds to 50% sulfur coverage] the corresponding calculations require 16 atoms per film unit cell.

At each of the three heights, we evaluated the total energy and electronic and magnetic structures self-consistently using six special k points. We further monitored the convergence with respect to k-point sampling of the total energies and work functions for the two heights, 1.09 and 1.14 Å, by performing self-consistent calculations using a 16 k-point mesh and the triangulation method due to Wang and Freeman[12] for evaluating the associated eigenvalue sums, charge densities, and work functions. We also used this method to construct DOS's for the electronic structure of the clean substrate, the isolated sulfur monolayer [with the spacing of the $c(2\times2)$ layer], and after adsorption with the S layer positioned at the height 1.14 Å. Because these calculations are based on the FLAPW method, there are no shape approximations assumed in the construction of the density or potential or in the solution of the associated eigenvalue problem anywhere in space. Core contributions are evaluated in the central field approximation fully relativistically. Valence contributions (which include the S 3s states located $\sim$1.3 Ry below the vacuum zero) are determined using the semirelativistic approximation near each atomic core and nonrelativistically in regions far away (in the vacuum and interstitial) from all cores. This is done through a variational solution of the FLAPW secular equations with a basis set consisting of between 950 and 1000 LAPW functions, corresponding to the choice of $Rk_{max}=7.5$, where $R=2.345\,580$ a.u. is the muffin-tin radius of each Fe sphere and k_{max} is the largest momentum component included in the basis set. Because z reflection is explicitly used to block diagonalize each secular matrix, the dimension required for each diagonalization actually only varies between 475 and 500. We used an angular momentum cutoff, $l_{max}=8$, for the augmentation of each plane wave to the radial functions at the boundary of each sphere. Nonspherically symmetric contributions to the density and potential were cutoff at the same l_{max} value. In the interstitial region, we used an RG_{max} value of 22. Here, G_{max} is the magnitude of the largest reciprocal-lattice vector included in the construction of the density and potential, where the reciprocal mesh parallel to the surface is defined by Fig. 1, with a bulk Fe lattice parameter of 5.4169 a.u., and the lattice parameter $\tilde{D}$ associated with the normal direction is 28.4192 a.u. This leads to an interstitial representation of the density and potential involving 1873 symmetrized star functions. In the two vacuum regions, which begin 12.5045 a.u. above and below the center of the film, warping contributions to the potential and density are derived using a mixed numerical-two-dimensional plane-wave representation in each of 100 equally spaced planes extending an additional 10 a.u. away from each boundary with 30 symmetrized star functions per layer. The remaining contributions to the density and potential in the vacuum region are evaluated using 250 equally spaced planes which extend outwards 25 a.u. from each vacuum boundary.

A significant saving in computational resources was made possible during these calculations by our application of the film-FLAPW Broyden method which we derived from the bulk procedure due to Singh, Krakauer, and Wang[13] for determining self-consistent solutions of the Kohn-Sham equations. In particular, we made use of an obvious generalization of the idea set forth by these authors, by modifying the existing (bulk) generalized Srivastava vector so that it includes one entry for each quantity associated with the vacuum. We explored various possibilities for reducing the size of the associated

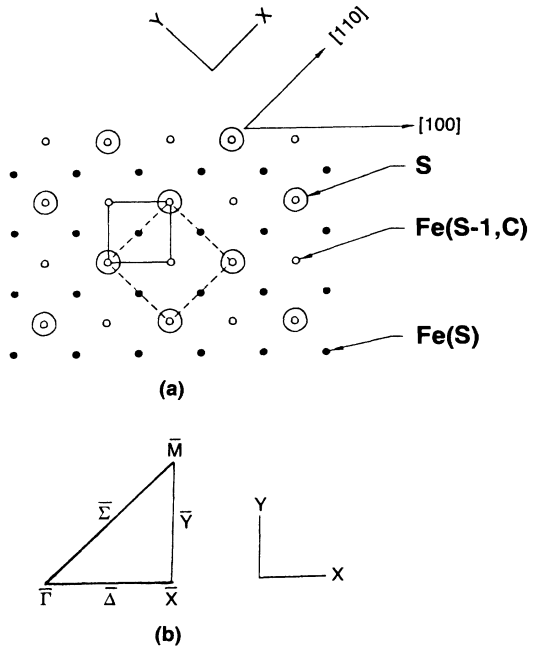

FIG. 1. (a) View from above of $c(2\times2)$ sulfur (S) chemisorbed on Fe(001); large open circles represent S atoms. Solid circles represent surface Fe [Fe(S)] atoms. Small open circles designate atoms in the first subsurface Fe [Fe($S-1$)] layer. Each Fe($S-1$) atom to the side of or under the S, throughout, respectively, is referred to by the same Fe($S-1,C$) or Fe($S-1,U$). The larger square, connected by dashed lines, shows the boundary of the two-dimensional unit cell appropriate to the $c(2\times2)$ coverage. The small square, connected by solid lines, shows the boundary of the comparable unit cell for the single atom per layer case, appropriate for the clean substrate. Also shown is the orientation of the crystallographic directions and the choice of coordinate system. (b) The irreducible wedge of the first surface Brillouin zone (SBZ) corresponding to the $c(2\times2)$ coverage, its orientation relative to our coordinate system, and the location of the high-symmetry points (found at the corners of the triangle) and symmetry lines.

Jacobian matrices, including omitting various quantities (such as the coefficients associated with the warping and non-muffin-tin contributions to the density) but found that only by including both the effects of vacuum warping and nonspherical variations in the density in the generalized vector were we able to achieve optimal efficiency from the method. We also achieved significant savings at the outset of the calculations by making use of an algebraic transformation[14] of the substrate density for the case of one Fe atom per layer to the unit cell involving two Fe atoms per layer.[7]

III. DETERMINATION OF EQUILIBRIUM HEIGHT AND WORK FUNCTION

The results of our energy minimization are summarized in Fig. 2, which shows the parabolic fit to our calculated values of the total energy (shown by crosses) as the height is varied. Our calculated minimum at $H_{eq}=1.12$ Å is in excellent agreement with the value [1.09(5) Å] derived by LJJM (Ref. 8) using a dynamical LEED intensity analysis. From this curve we also have extracted the first prediction of the perpendicular vibrational energy Ω, 45 meV. Provided the sulfur-induced relaxation of the outer Fe layers is insignificant [as we have assumed in our calculations, in accord with the findings of LJJM (Ref. 8)], independent verification by electron energy-loss spectrum experiments of the value of this quantity would provide an important test of the predictive power of our total energy calculations.

In Fig. 3, we have plotted the change in our calculated value of the work function as the height is varied, relative to our FLAPW-derived value, 4.45 eV, for the clean seven-layer Fe film. Experimentally (as noted above), Ueda and Shimizu found a slightly smaller change using the Fowler method,[6] ~0.55 eV, than our calculated equilibrium value, $\Delta\Phi_{eq}=0.86$ eV. The agreement, however, between our results (in which spin polarization is included) with these experimental results is considerably better than when spin polarization is ignored, as in the work of FW, where it is found that $\Delta\Phi$ is 1.3 eV.

It is interesting to note, furthermore, that a variety of experimental values for the work function of the clean surface have been found, ranging from 4.31 (Ref. 15) to 4.88 eV,[16] reflecting differences in sample preparation and experimental method. Since Shimizu and Ueda[10] base their measured change on the value 4.67 eV for clean Fe(001), it is apparent that roughly 70% of the difference (0.22 eV) between our calculated work-function change and their result reflects the difference between our respective values of Φ for the clean substrate. Thus our value of 5.31 eV and their result, 5.21 eV, for Φ after the chemisorption agree to within 0.10 eV.

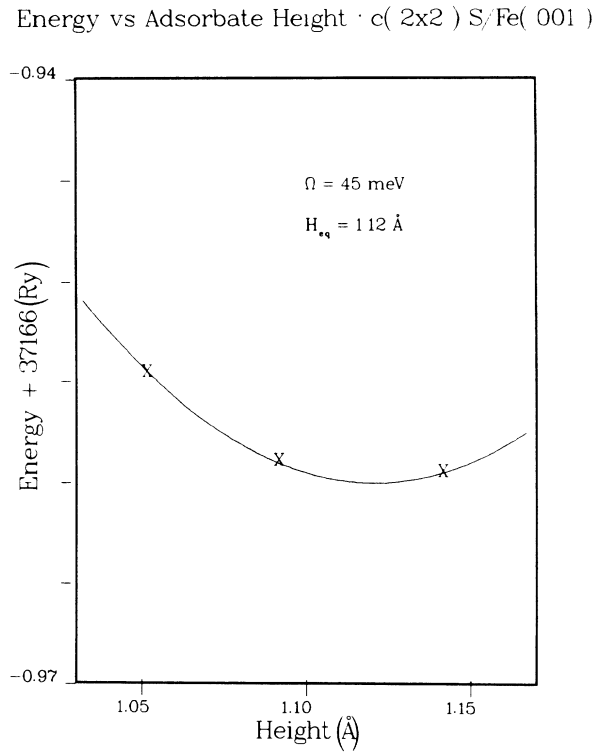

FIG. 2. Calculated total energies (crosses), and the parabolic fit to these values as the sulfur height is varied. H_{eq} denotes the value of the equilibrium height; Ω is the calculated perpendicular vibrational frequency.

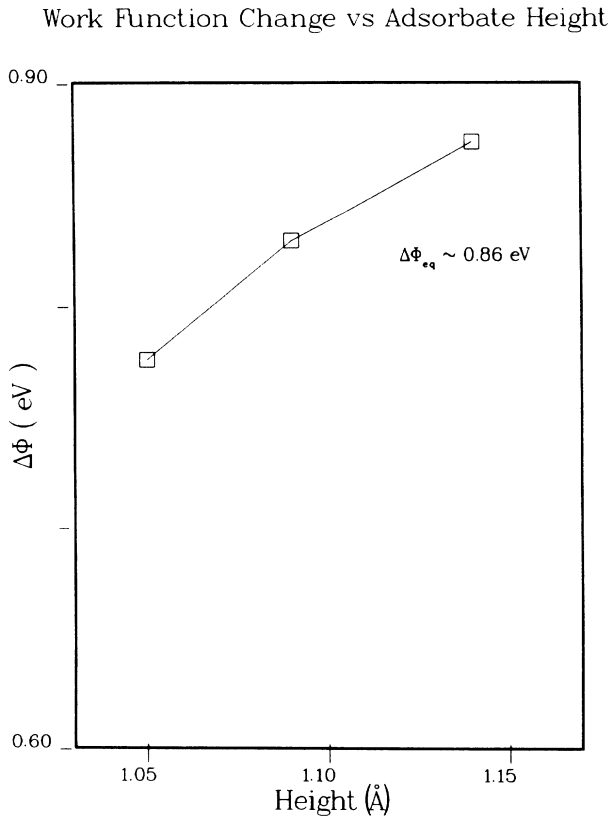

FIG. 3. The change in the calculated value of the work function as the height is varied, relative to the FLAPW derived value of the work function, 4.45 eV, for the clean seven-layer Fe film; $\Delta\Phi_{eq}$ is the extrapolated change at the calculated equilibrium height, $H_{eq}=1.12$ Å.

The considerably greater change in work function found in the paramagnetic calculations by FW (1.3 eV) than here (0.86 eV) is due to the much larger transfer of charge to the S atoms in the paramagnetic case. In Table I we have listed our calculated values for the minority, majority, and total valence charges of the various, independent atoms and the associated adsorption-induced changes in these quantities. For the case in which the sulfur height is 1.14 Å, we see that the adsorption leads to an increase of only 0.06 electrons on the sulfur atom, relative to a comparable sulfur atom within a free-standing, spin-polarized monolayer (with the same nearest-neighbor sulfur separations). FW found an increase of 0.23 electrons for the comparable increase. Part of this difference reflects the choice of a muffin-tin sphere size for the adsorbate: our sphere radius, 1.45 a.u., was chosen so that the sulfur could be moved arbitrarily closely to the Fe surface; FW's decision to use touching Fe-S spheres (with the S atom positioned 1.09 Å above the Fe plane) leads to a radius which is larger by about a factor of 2. However, by rescaling the charge transfers from our calculation by the ratio of the valence charges for the two cases, we still find that FW's calculated transfer is a factor of 2 larger than ours. This leads to the formation of a much larger adsorption-induced dipole layer of charge, with its electron end pointing away from the surface, which accounts for the considerably larger $\Delta\Phi$ value found by FW.

The values for the adsorption-induced changes in valence charge in the surface Fe [Fe(S)] and subsurface Fe($S-1$)...Fe($S-3$) atoms do not differ appreciably for the paramagnetic and spin-polarized cases. It is interesting to note, however, that a small shift of d charge within the first subsurface [Fe($S-1$)] atoms takes place, which does not seem to be present in the results of FW. This results from the formation of a majority bond involving hybridization of the $d(3z^2-r^2)$ states in the Fe($S-1,U$) atom, located below the S, with the bonding S(p_z) states. This bonding does not occur in the remaining [Fe($S-1,C$)] Fe atom and leads to a splitting (by $\sim 6\%$) in the magnetic moments (as discussed below) of the atoms in this Fe($S-1$) layer. This feature also shows that there is some participation of the subsurface d electrons in the chemisorption, which has been omitted in the analysis of photoemission line shapes by DPG.[9]

The surprisingly small transfer of charge to the S atom has interesting implications for the common, intuitive idea (cf. Ref. 10) that the large electronegativity of S is responsible for the poisoning of Fe as a catalyst as a consequence of charge transfer from the Fe to the S. In fact, the small change in work function is a clear indication that there really is not very much charge transfer involved. Indeed, FW argued that the large change in work function which they found (in disagreement with experiment) and the fact that the only important changes in the spectrum of eigenstates present in their calculations occur at energies greater than 5 eV below E_F suggest that the poisoning is indeed due to transfer of charge to the sulfur. Our results, on the other hand, not only reveal that charge transfer to the sulfur is really quite insignificant but that important changes in the distribution of charge in and around the Fe(S) and Fe($S-1$) atoms occurs, leading to the formation of counterpolarized arrangements of electrons which actually inhibit the increase of the work function and which involve modifications of d bonding. Furthermore, the associated charge transfers are markedly different for the majority and minority electrons.

The spatial distribution of the associated charge rearrangement in the (110) plane is shown in Fig. 4, where the difference between the densities of $c(2\times 2)$ S/Fe and the superposition of the free-standing monolayer (S) and

TABLE I. Total, majority, and minority valence charges, resolved by atom, and adsorption-induced changes in these quantities for (1) the free-standing substrate and isolated $c(2\times 2)$ adsorbate monolayer, labeled "clean," and (2) after adsorption, labeled "S/Fe," at the height, 1.14 Å. Fe(S) refers to the Fe atom in the surface layer; Fe($S-1$), Fe($S-2$), and Fe($S-3$) refer to the Fe atoms in the first, second, and third layers, respectively, below the surface. The independent atoms in the $S-1$ and $S-3$ layers are further distinguished by the letters U (for the atoms directly below the sulfur) and C. S refers to the sulfur atom.

	Fe($S-3$)		Fe($S-2$)	Fe($S-1$)		Fe(S)	S
	U	C		U	C		
			Majority charge				
S/Fe	4.66	4.65	4.71	4.65	4.71	4.65	0.93
Clean	4.66	4.66	4.72	4.68	4.68	4.87	1.17
Change	−0.00	−0.00	−0.01	−0.03	0.02	−0.22	−0.25
			Minority charge				
S/Fe	2.40	2.40	2.34	2.43	2.33	2.35	0.92
Clean	2.40	2.40	2.33	2.37	2.37	1.93	0.62
Change	0.00	0.00	0.00	0.06	−0.03	0.43	0.30
			Total charge				
S/Fe	7.05	7.05	7.05	7.08	7.04	7.00	1.85
Clean	7.05	7.05	7.05	7.05	7.05	6.79	1.79
Change	0.00	−0.00	0.00	0.03	−0.01	0.21	0.05

clean Fe film is plotted. The figure shows quite clearly the small transfer of charge and the associated dipole formation which is responsible for the small increase in work function. In particular the accumulation of charge immediately behind each sulfur atom is responsible for the increase. Note, however, that additional counterpolarizations of charge, involving the transfer of electrons to regions between the S and Fe(S) atoms take place. The associated dipoles act to *lower* the work function. The spatial distribution and orientation of the charge transfers shown in FW's Fig. 4 are similar to ours in the vicinity of the S and Fe(S) though the magnitudes of the transfers into regions both above and below the S do seem to be about a factor of 2 larger when magnetic effects are not included. It should be noted as well that there is a noticeable, though small, polarization of charge within the Fe($S-1,U$) atom located immediately below the S, which does not seem to be present in FW's Fig. 4. We will see that this last feature is largely due to the formation of a rather long-ranged Fe($S-1,U$)-S bonding, majority state, which results from the hybridization of Fe($d[3z^2-r^2]$) and S($p[z]$)-like electrons near the bottom of the majority Fe d bands.

Thus, not only is the charge transfer to the S rather small, the associated spatial distribution of the transfer is

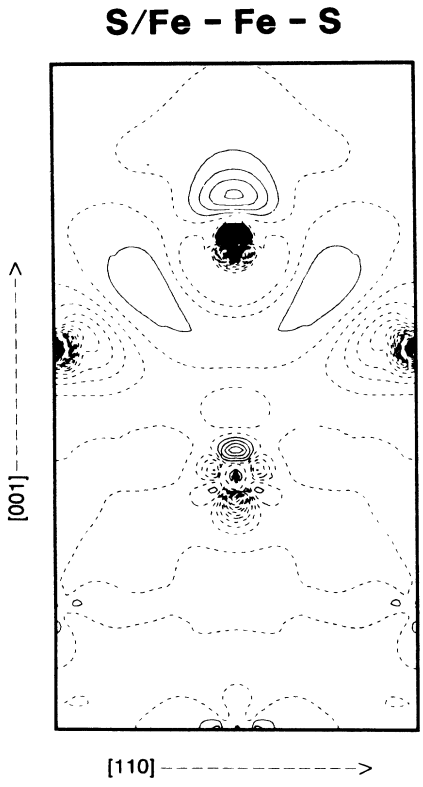

FIG. 4. Contour plot of the difference in the (110) plane between the valence density after adsorption and the superposition of the densities from the clean seven-layer Fe substrate and free-standing S monolayer possessing the spacing of the $c(2\times2)$ overlayer. Dotted lines throughout are used to label contours whose values are less than or equal to zero. Contours are linearly incremented in units of 0.005 e/a.u.[3]

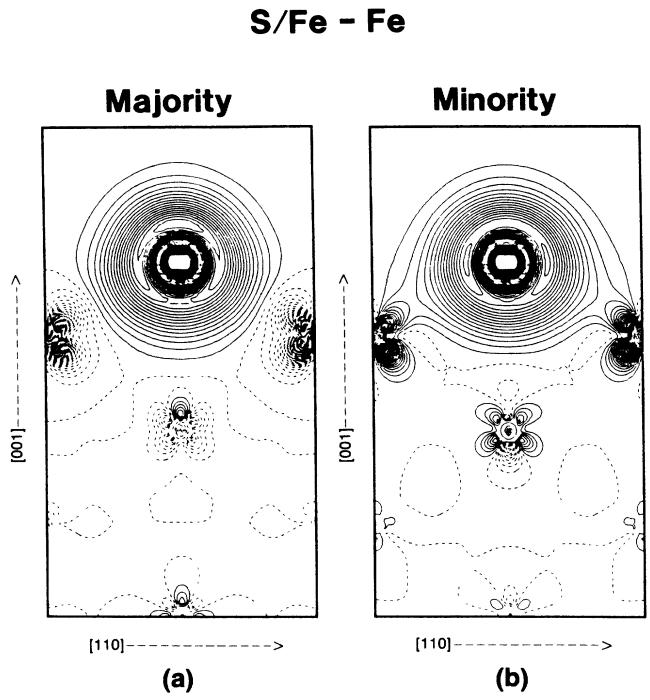

FIG. 5. (a) Contour plot of the difference in the (110) plane between the majority density after adsorption and the majority density of the clean substrate; (b) the comparable difference for the case involving minority densities; contours are linearly spaced as in Fig. 4. Note the strong S-Fe(S) bonding of the minority electrons and the lack of bonding in the majority electrons.

rather complicated. In addition, the redistribution of charge is strongly spin dependent. This is revealed by Fig. 5, which shows the difference between the valence densities of S/Fe and Fe for the majority (a) and minority (b) electrons. Note the very different behavior of electrons in the Fe(S) layer for the majority and minority cases. Specifically, in the minority case, $d[xy,yz]$-like lobed transfers into the region of each Fe(S) atom result, while the plot of the comparable transfer for the majority density difference reveals almost a mirror image of the transfer, involving $d[xy,yz]$-like losses of charge. This behavior leads to an important reduction in magnetic moment, which is discussed further in Sec. VI.

IV. DENSITIES OF STATES

In this section, we examine the origins of the charge transfers discussed in the last paragraph. We also examine the related modifications of magnetic and electronic structure through an analysis of the associated changes in the DOS's, and through contour plots of the energy-resolved spatial distribution of the density. We will also discuss the adsorption-induced changes of the unoccupied spectrum. This in turn will lead us to various inferences concerning the origins of the poisoning phenomenon, which we will discuss in the final section. We also identify and characterize the states associated with a prominent adsorption-induced splitting of Fe(S)-

like energy bands near E_F in the minority spectrum, which will be related in Sec. V to the behavior of states along the $\bar{\Delta}_2$ line of the surface Brillouin zone (SBZ) in the angle-resolved spectrum.

Figure 6 shows the spin-resolved local density of states (LDOS) for the various atoms before [Fig. 6(b)] and after [Fig. 6(a)] the adsorption. Included in Fig. 6(b) is the LDOS of the unsupported, magnetic sulfur monolayer possessing the lattice spacing of the $c(2\times2)$ overlayer. This figure reveals the adsorption induces (1) S-Fe(S)

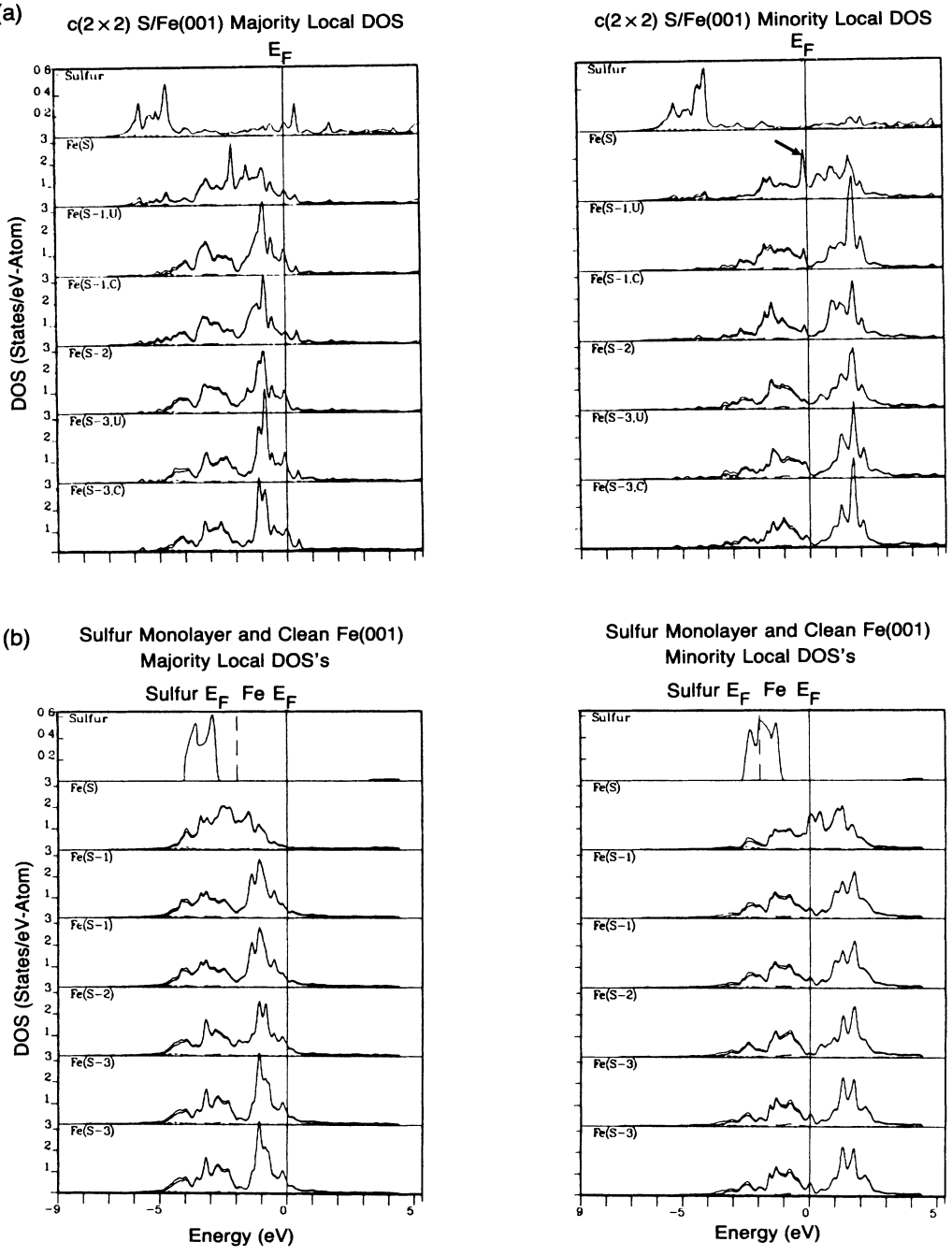

FIG. 6. Plot of the local densities of states (LDOS's), smoothed by Gaussian broadening (full width at half maximum is 0.05 eV), resolved by spin and atom after the adsorption (a) and for the clean substrate and unsupported sulfur monolayer (b); d-like and the sum of s-, p-, d-, and f-like contributions are both shown by solid lines. The short dashes are used to mark the s-like contributions, while the longer dashes indicate p-like contributions. The designations S, $S-1$, $S-2$, and $S-3$ are used to label the surface and subsurface layers, as in Table I. In the $S-1$ and $S-3$ layers, labels U and C are used to distinguish between Fe atoms located immediately under and to the side of the sulfur. The arrow to the right in Fig. 6(b) is used to mark the adsorption-induced, contamination sensitive minority peak.

bonding peaks centered at $E_F-5.5$ eV ($E_F-4.5$ eV) for the majority (minority) electrons, (2) important changes in the minority spectrum near E_F and in the unoccupied region, and (3) rather small changes in the exchange splitting between minority and majority Fe states (which remains large, ~ 1.2 eV). Furthermore, as we will see, because of this last feature (very little change in exchange splitting), the underlying involvement of the Fe d states in the first two sets of modifications is markedly polarized, involving majority d electrons in the formation of bonding peaks and minority d electrons near E_F and in the unoccupied region. This in turn leads to the strong spin dependence in the difference plots, discussed above.

The relatively small change in the exchange splitting associated with the Fe has an impact on the spin dependence of the resulting charge transfers which is reflected in the adsorption-induced shifts of the S-like peaks in the DOS relative to the iron d-like contributions. Specifically, in Fig. 6(b), we see that when the energy scales of the clean S and Fe LDOS's are positioned relative to the common electrostatic zero, the S majority peaks (which, as discussed further below, carry significantly greater weight than the minority peaks) are centered over a predominantly d-like region of the Fe majority DOS. The minority S peak, on the other hand, lies near the bottom of the Fe minority bands, where a noticeable, though small, s component contributes to the Fe LDOS's, and for the most part, the Fe LDOS is rather small. The adsorption leads to a clear broadening and downward shift of the S peaks in both the majority and minority LDOS's. Accompanying these changes in the sulfur LDOS is a noticeable broadening of the d-like components to the majority LDOS's of the Fe($S-1$) and Fe(S) atoms. In the minority spectrum, on the other hand, the most profound changes in the Fe-like contributions to the DOS for energies below E_F-2 eV occur in the Fe(S) atom and primarily involve s electrons.

These adsorption-induced changes in the Fe d states in the sulfurlike portion of the spectrum, as well as the resulting, strong spin dependence of the associated density (and charge rearrangement) are readily identified through energy-resolved plots. Specifically, in Fig. 7, we have plotted the logarithm of the majority [Fig. 7(a)] and minority [Fig. 7(b)] density (in 10^{-3} e/bohr^3) which results from the sum of all states between $E_F-8.3$ and $E_F-3.8$ eV. This corresponds to the region in which the

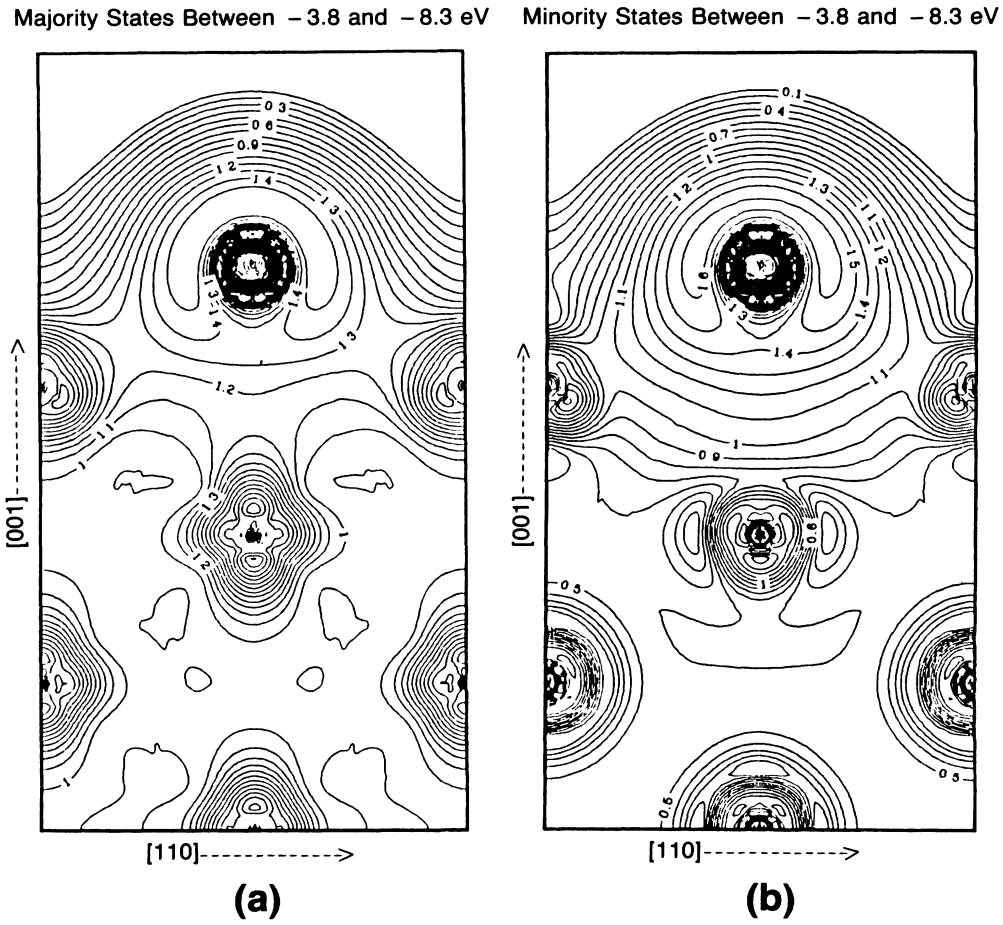

FIG. 7. Contour plot of the logarithm of the density (expressed in 0.001 e/a.u.^{3}) in the (110) plane associated with all of the (a) majority and (b) minority states with energies between $E_F-8.3$ eV and $E_F-3.8$ eV. Contours of the logarithm are linearly spaced in intervals of 0.1.

majority and minority LDOS's in the S atom are largest. A striking feature of the plot is that in this sulfurlike region of the spectrum, in which bonding occurs, a strong $d[3z^2-r^2]$-like spatial distribution is readily seen in the interior [Fe($S-1$)...Fe($S-3$)] layers in the majority density, while the minority density in this region is essentially s like. This feature is the source of charge transfer to the Fe($S-1,U$) atom which does not take place when magnetic effects are ignored (as discussed above). Near the Fe(S) atom also, the majority states from this energy region contribute considerably greater charge than do the minority states. The densities of both spins possess noticeable $d[xy,yz]$- and $d[xy]$-like character near the Fe(S) atom.

The changes in the Fe electronic structure in regions which have the greatest sulfurlike spectral weight lead to a broadening and downward shift of the Fe(S) d band (by ~ 1 eV), which in turn reflects a loss of states (~ 0.23 electrons) through charge transfer to the regions in and around the S. This behavior in turn leads to a lowering of the local electrostatic zero, and a downward shift of the minority bands takes place. It should be noted, however, that the resulting increase in minority charge, $0.43e$, which accompanies the shift is not the result of a simple band-filling effect, as Weinert and Davenport found for $p(1\times 1)$ H adsorbed on Ni,[4] in which the adsorption-induced loss of majority states through bonding with the adsorbate is matched by an approximately equal gain of minority states. We find, in agreement with FW, a net gain of ~ 0.23 electrons in each Fe(S) muffin tin, and that in this region, local charge neutrality is not preserved.

This last effect is not entirely unexpected. The $c(2\times 2)$ layer corresponds to 50% coverage of the surface and thus involves a considerably more open interface than $p(1\times 1)$ H/Ni(001). As a consequence, the accumulation of charge between the adsorbate and surface (as in Fig. 4), which occurs in regions near the adsorbate, is not as evenly distributed. Thus, the local electric fields vary less uniformly over the surface layer, and approximate neutrality within the surface layer during the adsorption is broken.

The downward shift of the minority spectrum associated with the gain of $0.43e$ in the Fe(S) atom is reflected by a prominent peak [marked by arrows in the minority portion of Fig. 6(a)] immediately below (but not at) E_F. This peak is absent from the comparable LDOS for the clean substrate Fe(S) atom, shown in Fig. 6(b). From Fig. 8, which shows the logarithm of the density in the (110) plane associated with this peak, we see that its angular momentum character is strongly $d[xy,x^2-y^2]$ and to a lesser extent $d[xz,yz]$-like in the Fe(S) and Fe($S-1$) layers. This feature is also seen in the band structures (as discussed further below). It is interesting to note as well that though non-negligible charge is associated with this peak throughout the Fe substrate, between the Fe($S-1$) and Fe($S-2$) layers, there is essentially a vanishing density, reflecting the antibonding nature of the states from this region of the spectrum.

Comparing Fig. 8 with Fig. 9, where the logarithms of majority [Fig. 9(a)] and minority [Fig. 9(b)] densities associated with the unoccupied states between E_F and $E_F+0.65$ eV are plotted, we see that the minority densities associated with states just below and above E_F both are strongly $d[xy,x^2-y^2]$-like throughout the film, but that above E_F, the $d[xz,yz]$-like character of the states is strongly reduced. The greater $d[xz,yz]$-like character of the occupied minority peak and the surprisingly large region over which the associated density is non-negligible (cf. Fig. 8) suggest that the transfer of minority states is largely of electrostatic origin.

Immediately at E_F, the LDOS in the minority for both the Fe(S) and Fe($S-1$) layers is actually reduced. In the occupied portion of the majority spectrum, the LDOS's for each of these two layers exhibits an upward shift (by ~ 0.25 eV), and each reveals a noticeable (though small) increase in value at E_F. Above E_F, on the other hand, there is a noticeable shift (towards the vacuum zero) and narrowing of minority states throughout the substrate but especially in the Fe(S) and Fe($S-1,U$) atoms [note the large peaks 2 eV above E_F in particular in Fig. 6(a)]. As a consequence, there is a considerable reduction in the total density of minority states (by 50%) at E_F for the entire film and especially for the Fe(S) and Fe($S-1,U$) atoms, while above E_F the region of appreciable DOS is much narrower and sharply peaked.

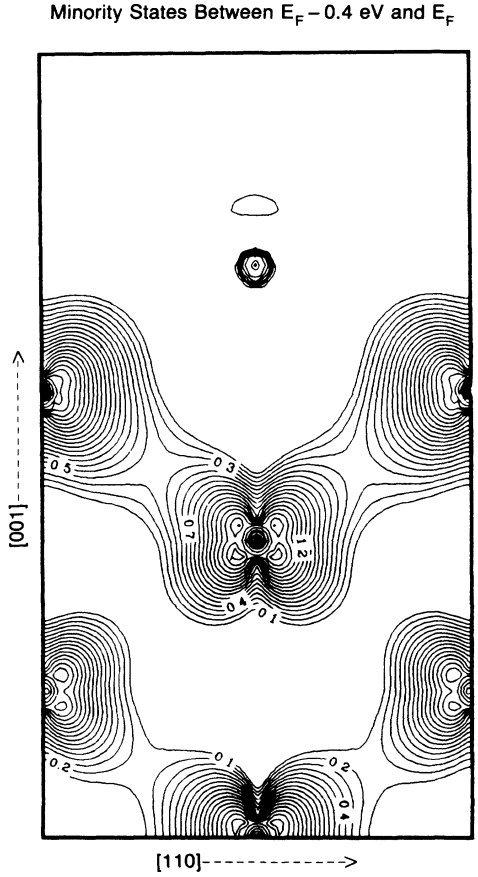

FIG. 8. Contour plot of the logarithm of the density (expressed in 0.001 e/a.u.^{3}) in the (110) plane associated with the minority states whose energies fall between $E_F-0.4$ eV and E_F. Contours are plotted as in Fig. 7.

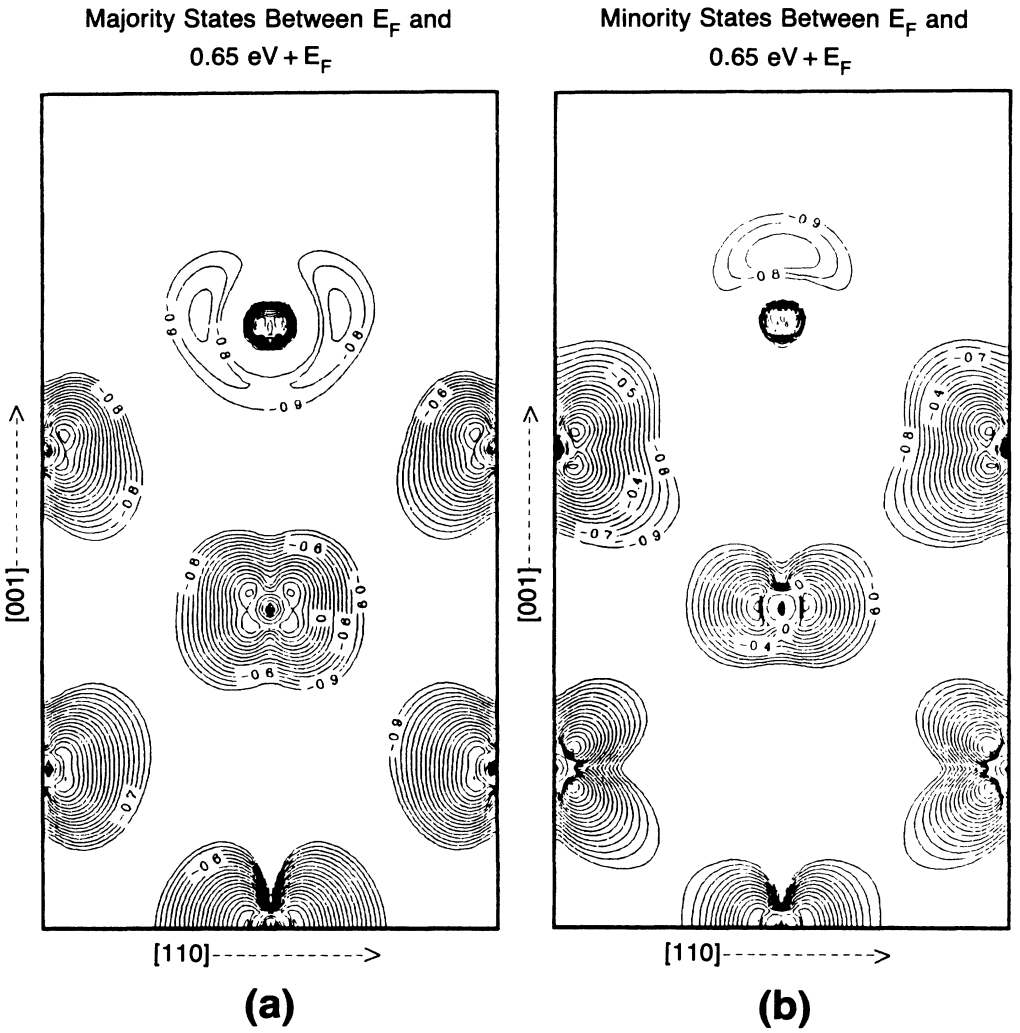

FIG. 9. Contour plot of the logarithm of the density (expressed in 0.001 e/a.u.^{3}) in the (110) plane associated with all of the (a) majority and (b) minority states with energies between E_F and $E_F+0.65$ eV. Contours are plotted as in Fig. 7. The lowest value of the logarithm is -1, here, as opposed to the value 0.1 found in Figs. 7 and 8.

V. ENERGY-BAND STRUCTURES

In Fig. 10, we have plotted the majority and minority band structures along the boundary of the $c(2\times2)$ SBZ before [clean Fe(001)] and after the adsorption. Here, bands are resolved by symmetry with respect to reflection though the plane normal to the surface containing the wave vector: states which are even (odd) with respect to this symmetry are shown in Fig. 10(a) [10(b)] and are also identified through the subscripts "1" ("2") beneath each point of high symmetry ($\bar{\Gamma}$, Σ, etc.). Also, dotted (dashed) bands are even ($+$) and odd ($-$) with respect to z reflection through the center of the film. The coloring of the bands distinguishes between states which have their largest muffin-tin charge within a particular sphere: respectively, bands which are colored red, yellow, green, aqua, or blue are to be associated with the S, Fe(S), Fe($S-1$), Fe($S-2$), or Fe($S-3$) sphere. Also plotted are results from the non-spin-polarized ARUPS experiments by DPG (Ref. 9) for the positions of the sulfurlike surface states (SS's) along the $\bar{\Gamma}$-$\bar{M}$ line.

As in the DOS, the most dramatic changes in the spectrum are the result of (1) the formation of sulfurlike bands between $\sim E_F-6.5(6.0)$ and $\sim E_F-4.5(4.0)$ for the majority (minority) electrons, and (2) the appearance of new, occupied and unoccupied Fe(S)-like minority states near E_F. The S-related surface bands are derived through important hybridization with Fe(S,d) and Fe($S-1,d$) states. This feature of the bonding was omitted from the earlier analysis due to DPG (Ref. 9) and also results in considerable ($\sim$0.5 eV) exchange splitting between the sulfurlike bands. This last feature leads to important, additional complications (discussed further below) which have been ignored previously.[9] The modifications near and above E_F, which may have bearing on the poisoning phenomena, enable us to make a variety of interesting predictions concerning the spectrum of occupied and unoccupied Fe-like bands which

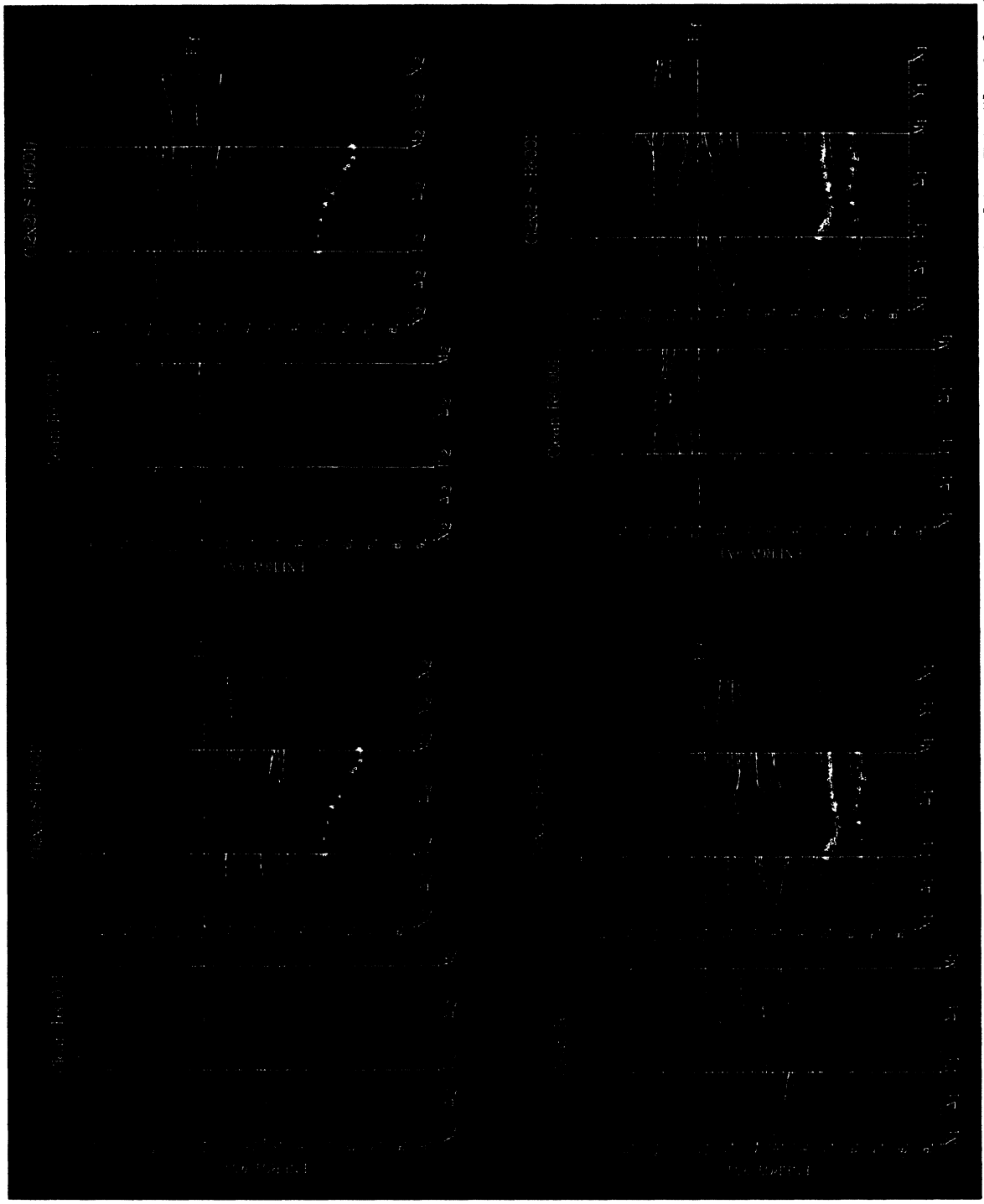

FIG. 10. The majority (left) and minority (right) band structures along the boundary of the $c(2\times2)$ SBZ, as defined in Fig. 1(b), before [clean Fe(001)] and after the adsorption; the clean Fe(001) bands are derived by folding back the spectrum for the SBZ of the single atom per layer unit cell (cf. Ref. 7). Bands are resolved by odd (even) symmetry with respect to reflection through the plane normal to the surface containing the wave vector, and denoted by the subscripts "2" ("1") beneath each point of high symmetry. Dotted (dashed) bands are even $(+)$ and odd $(-)$ with respect to z reflection through the center of the film. The coloring of bands distinguishes between states which have their largest muffin-tin charge within a particular sphere: respectively, red, yellow, green, aqua, or blue is to be associated with the S, Fe(S), Fe($S-1$), Fe($S-2$), or Fe($S-3$) sphere. Also plotted are results from non-spin-polarized angle-resolved UPS experiments by DiDio, Plummer, and Graham (Ref. 9) for the positions of sulfurlike surface states.

should be monitored through spin-polarized, ARUPS, and KRIPES experiments.

Specifically, in both symmetries ("1" and "2"), we readily identify the appearance of sulfurlike bands (shown in red). Since the experiments of DPG (Ref. 9) are non-spin-polarized, the comparison between experiment and theory is not without ambiguity. However, in the case of the majority spectrum, both the position (relative to E_F) and dispersion of our sulfurlike bands are in good agreement with DPG's findings for the S-derived "surface bands." In fact, our calculated $\bar{\Sigma}_2$ majority bands agree with the findings of DPG (Ref. 9) to within $\lesssim 0.1$ eV throughout the SBZ except very near $\bar{M}$, where the deviation is ~ 0.3 eV. The agreement with experiment for the $\bar{\Sigma}_1$ majority sulfurlike bands superficially would not appear to be quite as good. Here, in particular, we find the upper S band, which is $p[x,y]$-like at $\bar{\Gamma}$, is about 0.2 eV above the experimental value between $\bar{\Gamma}$ and $\frac{3}{4}\bar{\Gamma}$-$\bar{M}$, and agrees to within less than 0.1 eV for the remaining wave vectors along the Σ line. In place of the single lower SS found by these workers, however, we find a surface resonance, possessing strong sulfur character. This SR at $\bar{\Gamma}_1$ is defined by the two lowest, red bands, which have opposite z-reflection symmetry, and are split by ~ 0.5 eV. This majority resonance appears about 0.2 eV above the experimental data at $\bar{\Gamma}_1$.

In fact, as pointed out by DPG,[9] this band has overlap with the bulk Fe bands at $\bar{\Gamma}_1$, and neither falls within or at the boundary of a gap in the Fe bulk band structure. Thus, by definition, the state is a SR and not a SS. Its associated $p[z]$ character strongly affects this SR behavior and is responsible for the 0.5 eV splitting between the associated partner states of opposite z-reflection symmetry. This behavior is also consistent with the associated linewidth in the ARUPS intensity, where it was found by DPG (Ref. 9) that in the region of overlap with the bulk Fe band structure, the linewidth of the state is very large (~ 2 eV). Thus, the small disagreement of our calculated $\bar{\Sigma}_1$ majority S bands with experiment is readily accounted for by the resonant character of these states.

Comparison with the folded bands from the clean substrate reveals a variety of interesting, additional features about the nature of the lower $\bar{\Sigma}_1$ resonance. In particular, (1) at $\bar{\Gamma}_1$, the energy of the symmetric member of the SR essentially coincides with that of a $d[3z^2-r^2]$-like state possessing large Fe(S) and Fe($S-1$) components, (2) in the band immediately below this state, one also observes a strong Fe($S-1$)-like (green) component, while (3) after the adsorption, the comparable antisymmetric member of the SR band possesses large components in essentially all spheres (including the S). From these observations, we conclude that the lowest sulfurlike band is not well localized and evolves though a rather long-ranged interaction involving considerable hybridization with sp- and d-like Fe states over a wide energy range and over many layers.

As discussed by DPG,[9] one anticipates that this lower band would obtain greater localization near the sulfur in the region in which overlap with the Fe bulklike bands is reduced, which occurs at points between $\sim 0.5\bar{\Gamma}_1$-$\bar{M}_1$ and $\bar{M}_1$. And in fact, our calculated splitting between the two lowest (+ and −) $\bar{\Gamma}_1$ partner states becomes negligible near $\bar{M}_1$, indicating a true SS, and a noticeable sulfur (red) character begins to appear beginning at $\sim 0.6\bar{\Gamma}_1$-$\bar{M}$. However, this involves a shift of sulfur character from the third and fourth lowest $\bar{\Sigma}_1$ bands, which are associated with the SR at $\bar{\Gamma}_1$, to the lowest two states, providing still additional evidence for the resonant (as opposed to surface state) character of this sulfurlike band.

On the other hand, we also observe that though this lower band does fall below the bottom of the bands in the clean Fe substrate at $\bar{M}_1$, has noticeable sulfur (red) character and is a well-defined SS, it does possess blue [Fe($S-3$)], green [Fe($S-1$), and yellow [Fe(S)] components. Comparison with the bands from the clean substrate further reveals that this admixture of components from all of the spheres appears at precisely the point at which the SR crosses the boundary ($\sim 0.6\bar{\Gamma}_1$-$\bar{M}_1$) of the bulk bands, indicating that the SS, though localized near the S, has evolved out of considerable hybridization with Fe states from thoughout the film. In our earlier discussion of the energy-resolved density from the sulfurlike bands, we further identified an important $d[3z^2-r^2]$ component in the majority density, throughout the film, which (as revealed by Fig. 4) results largely from states near the energy of this band. These observations imply that considerable mixing of states, over many layers, is involved in the evolution of this surface state, and that the hybridization depends strongly on k parallel ($k_\parallel$), even at values of $k_\parallel$ in which the overlap of the Fe bulk bands with the S band becomes negligible. This observation in turn suggests that the measured sensitivity with respect to changes in $k_\parallel$ of the linewidths associated with this SS could be due to initial-state effects and not to a more subtle final-state mechanism in which "bulk $3d$ states ... hybridize with surface 2D states even when they appear to be separated in E-$k_\parallel$ space," as inferred by DPG.[9]

It should be noted as well, however, that because of the ~ 0.5 eV exchange splitting and the fact that our majority states agree well with experiment, we find fairly large differences between our calculated $\bar{\Sigma}_1$ and $\bar{\Sigma}_2$ minority sulfurlike bands and those derived from these experiments, which suggests that the experiment has preferentially sampled majority states. It is also possible that the large linewidths associated with these measurements by DPG (Ref. 9) are partly the result of the exchange splitting. The large exchange splitting of these sulfur states provides an additional complication in the analysis of linewidths which these authors did not consider. Clearly, spin-polarized ARUPS measurements would clarify our interpretation of these results.

Because the type-2 sulfur states are $p[x,y]$-like, they remain as well localized surface states below and at the boundary of the Fe bands along all of the symmetry lines. We have already seen that along the $\bar{\Sigma}_1$ line, the $p[z]$ character of the lower $\bar{\Gamma}_1$ sulfur band results in strong hybridization with the Fe states, which in this energy range in the clean substrate are primarily nearly-free-electron-like and bulklike. Between $\sim 0.7\bar{\Gamma}_1$-$\bar{M}_1$, where the overlap between the lower S band and Fe bands becomes negligible, and $\bar{M}_1$, this $p[z]$-like character is transferred

from the lower band, which becomes a well-defined sulfur SS, possessing entirely $p[x,y]$-like character in the S sphere at $\overline{M}_1$, to the higher band, which loses its predominantly sulfurlike component but remains highly localized in the Fe(S) layer. Between $\overline{M}_1$ and $\sim 0.4\overline{M}_1$-$\overline{X}_1$, these $\overline{Y}_1$ states, which are the lowest in energy in Fig. 10 along this symmetry line, gradually lose their surface state character and become resonances, a feature readily identified by the pronounced splitting (~ 0.25 eV) between z-reflection partner states which is found at $\overline{X}_1$. Along the $\overline{\Delta}_1$ line, this splitting becomes even more pronounced, and S and Fe(S)-like character is transferred to the six lowest $\overline{\Delta}_1$ bands as the S-like states overlap with the predominantly bulklike Fe s band. Thus, in the bonding region, the most pronounced sulfurlike SS's are found in the symmetry-2 bands all along the boundary of the SBZ and in the symmetry-1 bands along the $\overline{\Sigma}$ and $\overline{Y}$ lines near $\overline{M}$.

In the remaining portions of the occupied majority and minority spectrum, except very near E_F the adsorption induces rather subtle changes. These are largely accounted for by the presence of avoided crossings which result as a consequence of the reduced symmetry of the SBZ after the chemisorption.

Near E_F in the majority bands, the adsorption-induced loss of charge in the Fe(S) atom leads to a narrowing and upward shift of the yellow, Fe(S)-like bands, as a consequence of the contraction of the Fe(S) d states. This leads to the formation of an adsorption-induced $\overline{\Delta}_1$-$\overline{\Sigma}_1$ Fe(S)-like SR state. This state is the lowest unoccupied state at $\overline{\Gamma}_1$, where it is $d[xz,yz]$-like. It strongly hybridizes with states in the Fe($S-1$) and Fe($S-2$) layers along the $\overline{\Delta}_1$ line, essentially becoming bulklike at the point, $0.5\overline{\Gamma}_1$-$\overline{X}_1$, where it crosses E_F. Along the $\overline{\Sigma}_1$ line, the state remains strongly Fe(S)-like above E_F, and after it becomes occupied (at $\sim 0.5\overline{\Gamma}_1$-$\overline{M}_1$), it begins to mix strongly with bulk Fe-like bands in the immediate vicinity of $\overline{M}_1$, where it loses its Fe(S)-like character. A similar majority $\overline{\Delta}_2$-$\overline{\Sigma}_2$ SR state is induced. The antisymmetric member with respect to z reflection of this SR is the lowest unoccupied ($-$) $\overline{\Delta}_2$ and $\overline{\Sigma}_2$ band. At $\overline{X}_2$, this band has its strongest Fe(S)-like character. Beginning at $\sim 0.7\overline{X}_2$-$\overline{\Gamma}_2$, the splitting between its $+$ and $-$ partners becomes so large that the ($+$) member becomes occupied, suggesting that important coupling to bulk states in this resonance may inhibit its detection through KRIPES measurements except between $\overline{X}_2$ and $\sim 0.7\overline{X}_2$-$\overline{\Gamma}_2$. There are interesting, additional transfers of Fe(S)-like character to most of the bulk nearly-free-electron-like unoccupied $\overline{\Sigma}_1$ and $\overline{\Sigma}_2$ bands, as well as the appearance of sulfur 4s-like character in the $\overline{\Sigma}_1$ state near $\overline{\Gamma}_1$ (at ~ 2.5 eV) and the $\overline{\Delta}_1$ state which crosses $\overline{X}_1$ at ~ 4.2 eV.

Because of their relevance of the poisoning phenomenon, the most interesting adsorption-induced changes in the band structure occur in the minority spectrum, above and immediately below E_F. Here, we find a pronounced, flat SS-SR, is induced all along the $\overline{\Delta}_2$ line just below E_F. This band crosses $\overline{X}_2$ at ~ -0.15 eV as a SS possessing $d[xz,yz]$-like character and remains a SS along most of the $\overline{\Delta}_2$ line, becoming a SR only after it begins to overlap with bulk bands near $0.9\overline{X}_2$-$\overline{\Gamma}_2$. It crosses $\overline{\Gamma}_2$ at ~ -0.20 eV where again it is entirely $d[xz,yz]$-like. Comparison with the clean substrate reveals that this band is induced through level repulsion of two highly localized $\overline{\Delta}_2$ SS's, which are degenerate at $\overline{X}_2$ (i.e., at $0.5\overline{\Gamma}_2$-$\overline{M}_2$ relative to the unfolded SBZ of clean substrate) with energy ~ 0.1 eV. Along the $\overline{\Delta}_2$ line, these two, folded bands remain unoccupied until $\sim 0.55\overline{X}_2$-$\overline{\Gamma}_2$, where the lower band crosses E_F, hybridizes with the Fe($S-1$) $d[xz,yz]$-like states and immediately loses its Fe(S)-like character. The adsorption induces a large Fe(S) component in the continuation of this band along the $\overline{\Sigma}_2$ line, which is absent from the clean substrate, where the state has its largest component in the Fe($S-1$) sphere. Immediately above this band, we find a sulfur-induced downward shift of a second, symmetry-2 Fe(S) band. At $\overline{\Gamma}_2$, this state, which is less than 0.05 eV below (above) E_F after (before) the adsorption, is entirely $d[x^2-y^2]$. After the adsorption, this band remains primarily below E_F along $\overline{\Sigma}_2$, while in the clean substrate, it remains unoccupied over a considerably larger range of wave vectors.

Because (1) these $\overline{\Delta}_2$-$\overline{\Sigma}_2$ bands become occupied in precisely the same energy range and have the identical angular momentum composition as the sulfur-induced $d[xy,x^2-y^2]$- and $d[xz,yz]$-like states associated with the peak in the minority Fe(S) LDOS just below E_F (marked by arrows in Fig. 6), and (2) the important changes in the minority symmetry-1 bands occur in a different energy range, we infer that the occupation of these highly localized, Fe(S)-like symmetry-2 bands is closely associated with the appearance of this peak. Furthermore, having made this identification, we further note that the level repulsion of the two $\overline{X}_2$ unoccupied surface states from the clean Fe substrate, which leads to the extremely flat sulfur-induced Fe(S) $\overline{\Delta}_2$ SS, also results in the lowering below E_F by ~ 0.15 eV of an extremely flat band, which, for the clean Fe, essentially maintains a constant energy that falls within ~ 0.01 eV of E_F over a large range of wave vectors along the $\overline{\Delta}$ line. This behavior suggests that the sulfur-induced reduction in the DOS at E_F [especially in the Fe(S) atom] is strongly correlated with the level repulsion of these unoccupied $\overline{\Delta}_2$ bands. Thus, independent verification of our predictions of the sulfur-induced occupation of the $\overline{\Delta}_2$ and $\overline{\Sigma}_2$ bands and the significant increase in energy (~ 1 eV) of the lowest unoccupied minority $\overline{X}_2$ minority state through spin-resolved ARUPS and KRIPES measurements would provide an important test of our calculated electronic structure, the behavior of minority states near E_F, and reduction in the DOS at E_F. Because we draw various inferences below related to the poisoning phenomenon which are closely tied to these results, verification of these adsorption-induced features could have important implications for understanding the interplay of S with Fe in various catalytic processes.

Independent verification of various adsorption-induced features in our results for the unoccupied minority spectrum away from E_F also would provide an important test of implications concerning the poisoning. In particular, at $\sim 2.70(25)$ eV above E_F, we find three sulfur-induced,

unoccupied Fe(S)-like SR's at $\bar{\Gamma}$. (The large energy uncertainties reflect the large splittings between partner states of different z-reflection symmetry.) Two of these are continuations of $\bar{\Sigma}_1$ resonances. The remaining SR has symmetry 2. All of these SR's maintain some Fe(S) character between $\bar{\Gamma}$ and $\sim 0.5\bar{\Gamma}$-$\bar{M}$. Between $0.5\bar{\Gamma}$-$\bar{M}$ and $\bar{M}$, the lower $\bar{\Sigma}_1$ SR beings to hybridize with bulk states, while the upper $\bar{\Sigma}_1$ SR becomes more pronounced. Both sets of bands cross $\bar{M}_1$ at ~ 2.4 eV. The $\bar{\Sigma}_2$ SR, which is $d[xz,yz]$-like at $\bar{\Gamma}_2$, mixes strongly with bulk states and with the continuation of the highest occupied band, which has considerable Fe(S) character at $\bar{\Gamma}_2$ but acquires large bulk components near $0.2\bar{\Gamma}_2$-$\bar{M}_2$. As a consequence, this SR becomes delocalized beyond $0.5\bar{\Gamma}_2$-$\bar{M}_2$. Along $\bar{\Delta}$, on the other hand, the continuation of the SR possessing type-2 symmetry becomes sharper and remains highly localized all along the line, crossing $\bar{X}_2$ at ~ 2.3 eV, while the symmetry-1 SR's both acquire large bulk components very near $\bar{\Gamma}_1$. At $\bar{\Gamma}_1$, we also find an Fe(S)-like SR ~ 0.2 eV below the vacuum zero. This SR remains predominantly Fe(S)-like along $\bar{\Gamma}_1$-$\bar{X}_1$ and also acquires a sulfur 4s component between $\sim 0.4\bar{X}_1$-$\bar{\Gamma}_1$ and $\bar{X}_1$. The set of bounds associated with this SR crosses $\bar{X}_1$ ~ 0.5 eV below the vacuum zero.

VI. MAGNETISM

As noted in the last two sections, the adsorption induces a new, Fe(S), minority, occupied peak, just below E_F, through hybridization and level repulsion between Fe(S) $d(xz,yz)$-like SS's located just above E_F, near $\bar{X}_2$ prior to the adsorption. This is responsible for a large increase in minority occupation in the Fe(S) atom. The resulting gain of 0.43 minority electrons is accompanied by a loss of 0.22 majority electrons, resulting in a reduction by $\sim 20\%$ ($0.65\mu_B$) in the Fe(S) moment (see Table II). As a consequence, the moment of this atom becomes very nearly equal (to within 2%) to the moment of bulk Fe ($\sim 2.26\mu_B$).

As noted in Secs. IV and V, the net decrease in d states by the Fe(S) atom indicates that this behavior is not a simple electrostatically driven band-filling effect, in which the adsorption-induced loss of majority states through bonding with the adsorbate is matched by an approximately equal gain of minority states, but that the large exchange splitting in Fe plays an important role in the resulting adsorption-induced reduction in moment. In fact, the decline in the total DOS at E_F and the adsorption-induced level repulsion (as well as the resulting occupation by states just below E_F) in the minority spectra are clear indications that important changes in the electrostatic and exchange correlation potentials are at work which complicate the effect. However, especially away from E_F in the occupied region of the spectrum, the induced upward (downward) shifts of majority (minority) Fe(S) states do indicate that a band-filling-like mechanism is at work. In particular, the loss of majority Fe(S) states, which reflects an antibonding hybridization between the majority Fe(S) $d[xz,yz]$-like bands and the occupied and unoccupied sulfur $p[z]$ majority states, leads to a decrease of the local electrostatic potential and a binding of minority states.

The unoccupied S $p[z]$ states which play an important role in the loss of majority states appear in the minority spectrum of the unsupported S monolayer but reside in the majority spectrum after the adsorption (cf. Fig. 6). The shift of these unoccupied S states from minority to majority cannot be verified by experiment since an unsupported S monolayer is not physically realizable. On the other hand, the underlying physics reflects an interesting feature of S, which is not commonly recognized. According to local-density theory (as verified by direct calcula-

TABLE II. Calculated B_{HF} in kG (total), contributions to B_{HF} from valence and core electrons, and magnetic moments (μ_B) resolved by layer and atom and the associated adsorption-induced changes in these quantities. The labeling of atoms and the designations "Clean" and "S/Fe" are defined in Table I.

	Fe($S-3$)		Fe($S-2$)	Fe($S-1$)		Fe(S)	S
B_{HF}	U	C		U	C		
				Total			
S/Fe	−372	−352	−325	−344	−379	−254	7
Clean	−383	−383	−325	−406	−406	−246	−33
Change	12	31	0	62	27	−8	39
				Valence			
S/Fe	−83	−58	−22	−59	−75	41	8
Clean	−87	−87	−13	−103	−103	147	62
Change	4	30	−10	43	28	−106	−54
				Core			
S/Fe	−289	−294	−303	−285	−304	−295	−1
Clean	−296	−296	−313	−303	−303	−393	−95
Change	7	2	10	18	−0	97	94
				Moments			
S/Fe	2.26	2.25	2.37	2.23	2.37	2.30	0.00
Clean	2.26	2.26	2.39	2.32	2.23	2.94	0.55
Change	−0.00	−0.00	−0.03	−0.09	0.06	−0.64	−0.55

tion[17]), as an isolated atom, S possesses a magnetic moment of $2\mu_B$, and this is also the moment for each unit cell in the unsupported monolayer. [Indeed, within the muffin tin of the S (whose radius in these calculations is 1.45 a.u.), the moments of the isolated atom ($0.60\mu_B$) and in the monolayer ($0.55\mu_B$) are nearly equal.] The shift of the unoccupied S[p] states then reflects a stabilizing of the paramagnetic state of the atom after the adsorption and leads to the adsorption-induced loss of majority and gain of minority states responsible for a vanishing of the moment on the S after the chemisorption.

As noted above, there are small, though noticeable changes in the moments of the two Fe($S-1$) atoms. Specifically, the Fe($S-1,U$) atom, which is located directly below the S, loses majority $d[3z^2-r^2]$ electrons through hybridization with the occupied S $p[z]$ states. The remaining majority and minority d states on this atom contract in response, leading to net gains (by 0.03 electrons) in total charge and (by 0.06 electrons) in minority occupation. Thus, the moment on this atom decreases by $\sim 0.10\mu_B$. These changes within the Fe($S-1$) layer have further effects on the local electrostatic and exchange-correlation potentials which lead to a small gain (0.02) in majority occupation and loss (0.03) of minority states in the remaining Fe($S-1,C$) atom. As a consequence, the moment on this atom increases by a small ($0.06\mu_B$) amount. The end result is that the moments of the two Fe($S-1$) atoms, which are equal in the clean adsorbate, are split by about 6%. Similar behavior occurs when $c(2\times 2)$ O chemisorbs on Ni(001).[18] In both cases, these changes in magnetism within the interior of the substrate are manifestations of changes in the d bonding. [The identification of this feature has consequence because it has been assumed both in $c(2\times 2)$ S/Fe(001) and in $c(2\times 2)$ O chemisorbed on Ni(001) that changes in d bonding are negligible either beyond the surface layer[19] or throughout the substrate.[9]] In the remaining Fe atoms, the adsorption-induced changes in the magnetic moments are negligible.

In Table II, we have also listed the contact hyperfine fields $B_{\rm HF}$ for the various atoms, the adsorption-induced changes in these quantities, and the associated contributions from the valence and core electrons. As described elsewhere,[3] layer resolved measurements of $B_{\rm HF}$, in principle, can provide an important check on the accuracy of our calculations. Though in the current chemisorption the lack of symmetry between atoms within the $S-3$ and $S-1$ layers makes it somewhat difficult to compare the numbers found in Table II with such layer resolved experimental measurements, in the case of the $S-1$ layer, the adsorption induces a measurable isomer shift Δv (~ 0.05 mm/sec) on the Fe($S-1,C$) atom which is considerably greater (by a factor of ~ 10) than our calculated (negligible) value of Δv for the remaining [Fe($S-1,U$)] atom. This is fortunate because the largest changes in $B_{\rm HF}$ occur in the Fe($S-1$) layer, where the adsorption induces increases of 62 (27) kG for the Fe($S-1,U$) [Fe($S-1,C$)] atoms. The different values of Δv for the atoms in this layer should lead to resolvable shifts of the centroids of the associated Mössbauer peaks, and, as a consequence, it should be possible to distinguish between the values of $B_{\rm HF}$ for the two Fe($S-1$) atoms. For the Fe(S) and Fe($S-2$) atoms, where results from measurements of $B_{\rm HF}$ can be compared directly with our findings, we find that the adsorption induces small changes. In the case of the Fe(S) atom, this behavior reflects a surprising cancellation, involving a large contribution from the change due to the valence electrons ($+106$ kG) which is effectively canceled by a large change (-97 kG) from the core electrons.

VII. POISONING

To understand completely the origins of the sulfur-induced poisoning of the catalytic value of Fe in, for example, the Fischer-Tropsch synthesis of hydrocarbons, it would be necessary to perform a series of calculations which incorporate the constituent materials associated with the specific process, with and without small amounts of a sulfur contaminant. This of course is a formidable task, which would involve calculations that are considerably more difficult to perform than the ones discussed here. Nonetheless, there are a variety of adsorption-induced features that are readily apparent from our calculations which could have bearing on the poisoning phenomenon.

In the preceding sections, we have found that the adsorption induces important changes near the Fermi level in the minority spectrum as well as changes above E_F, and that only a rather small transfer or charge to the sulfur atom is involved. FW, on the other hand, in their paramagnetic calculations found the adsorption induces very little change in the DOS's except at energies below E_F-4 eV, and a rather large change in the work function through a considerably larger charge transfer to the S. We have further identified that the very different behavior we found is closely associated with level repulsion of unoccupied minority Fe states, near $\bar{X}_2$, and above E_F. Because our results for the change in work function and positions of bonding sulfurlike states are in considerably better agreement with experiment, we conclude that the behavior associated with the minority states in particular has an important impact on the sulfur-derived changes in electronic structure, and as a consequence that magnetism plays a critical role in these changes, and, by inference, in the poisoning.

More specifically, we suggest that the poisoning phenomenon is closely tied to (1) the appearance of the prominent minority peak immediately below E_F which is split from the next (unoccupied) peak, (2) appreciable reduction (by 50%) in the minority (as well as the total) DOS at E_F, and (3) a shift (towards the vacuum zero) and narrowing of unoccupied minority states throughout the substrate but especially in the Fe(S) and Fe($S-1,U$) atoms. These changes reflect rather important differences in the regions of the DOS which not only could be involved in the bonding of (e.g. CO) electrons during the intermediate stages of a catalytic process but which provide an important component to the final-state distribution of states in the determination of the rate of a particular reaction (as discussed further below). We suggest that the poisoning is indeed related to the loss of

minority states at E_F and the effective decrease in width of unoccupied states, and not to a large transfer of charge from the Fe to the S, as was inferred by FW.

This type of argument is not new. Feibelman and Hamann[20] have argued on the basis of electronic structure calculations involving a catalyst (rhodium) and a sulfur poison that the reduction in the DOS at E_F which they find in their calculation should play a prominent role in the poisoning of Rh as a catalyst. In the case of Fe, we find a similar reduction, but we also have observed the reduction is intimately related to the behavior of the minority spectrum, and thus tied to magnetic ordering, through the large exchange splitting in Fe.

Feibelman and Hamann have used the spatially resolved DOS at E_F and a Fermi golden-rule-type argument to infer that their calculation has bearing on the poisoning phenomenon. We wish to point out that the same Fermi golden-rule-type argument suggests that calculated changes in the DOS both at and *above* E_F of model systems such as ours (in which only the catalyst and poison are included) may have bearing on the poisoning. This is because, especially near the Fe surface, the unoccupied states play a prominent role during the intermediate stages of a catalytic process. The importance of these states in a Fermi golden-rule expression for the transition rate of a particular reaction is manifested both through matrix elements and through the final-state distribution of the ground state of the catalyst. In such an expression, the relevant final-state wave functions and density of states should be derived in the limit in which the Fe [S/Fe] catalyst is moved infinitely far from the other participants in the reaction.

In Fig. 11, we have plotted the spatially resolved difference between the density associated with the unoccupied states after and before the adsorption. Disregarding the energy dependence of matrix elements associated with any specific catalytic process, we may infer from this plot that the definite shift of states *away* from the surface region into the substrate which is induced from the sulfur should lead to a significant reduction in overlap between states from a molecule (such as CO) colliding with the Fe surface with the unoccupied Fe(S) states nearest to the surface. The origin of this behavior is closely associated with the narrowing of states in the peaks 2 eV above E_F. As a consequence, we infer that the changes in these states probably are related to the poisoning.

In fact, in the actual case of the hydrogenation of CO on an Fe surface, it is believed[21] that CO chemisorbs disassociatively through an intermediate molecular state, in which 4Σ and 1π orbitals from the CO are thought to form Fe—C-like bonds through a hybridization involving unoccupied Fe states, and electrons from occupied Fe states are backdonated into the antibonding $2\pi^*$ (oxygen-like) orbitals. As a consequence, the presence of the Fe leads to an elongation of the CO bond and dissociation, thus enhancing C-H formation. The poisoning of the reaction then involves disruption of one or both of two features associated with this elongation of the C—O bond: (1) the formation of the Fe—C-like bond, and (2) backdonation of Fe electrons towards the O.

The first of these features (1) is closely tied to the behavior of the uncoupled minority states. We infer from Fig. 6 that the most important changes in the unoccupied minority spectrum occur ~ 2 eV above E_F. Because this occurs at an energy (~ -2.45 (~ -3.31) for Fe [S/Fe] relative to the vacuum electrostatic zero) very close to the observed splitting between 1π and 4Σ levels in the gaseous CO molecule (2.75 eV), we suggest that the adsorption-induced lowering (~ 0.86 eV) in absolute energy and the associated narrowing and localization of the Fe(S)-like component in these states is probably closely tied to the weakening of the C—Fe bond. Thus, the weakening of the C—Fe bond would seem to be closely associated with the S-induced shift of states away from the Fe surface.

The second feature (2), involving backdonation of Fe electrons, is more closely tied to the behavior of the states at and immediately below the Fermi level. Especially through our analysis of the band structures, we have found that though the adsorption-induced downward shift in absolute energy of the minority states near E_F is small in magnitude, an important level repulsion is involved. Because the magnitude of the accompanying, upward repulsion of unoccupied states (especially near $\bar{X}_2$) is as large as 1 eV, both features (1) and (2) are closely

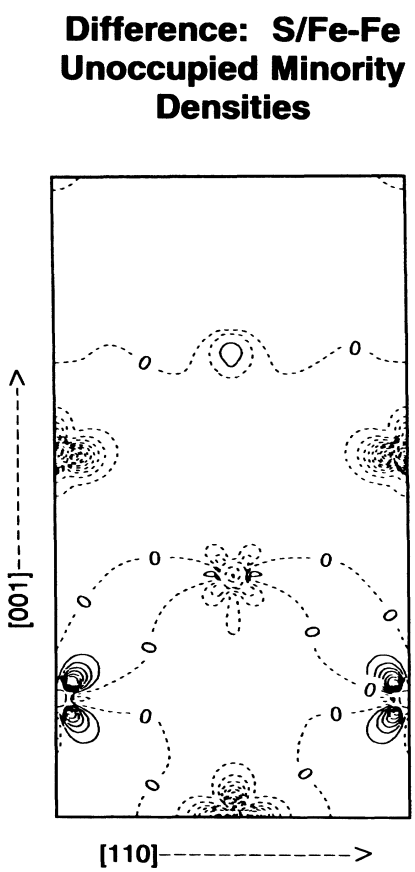

FIG. 11. Contour plot of the difference in the (110) plane between the density associated with all of the unoccupied states after adsorption and the comparable density from the clean substrate. Contours are plotted as in Fig. 4 but with a spacing of 0.0005 e/a.u.^{3}

tied to the behavior of the minority states near E_F.

The accuracy of these predictions and inferences could be monitored through the direct measurement of spin-resolved UPS, ARUPS, IPS, and KRIPES majority and minority spectra. In particular, there should be clearly resolvable increases (decreases) in majority (minority) spectra at E_F, as well as the appearance of small, adsorption-induced majority peaks about 0.5 eV above E_F. A contamination induced splitting of minority states at $\bar{X}_2$ of the highly localized $d[xz,yz]$-like Fe(S) SS, located ~ 0.1 eV above E_F in the clean substrate, should be readily observable. A pronounced d-like narrowing should be present at about 1.8 eV above E_F in the unoccupied, minority spectrum, and a pronounced peak just below E_F should develop.

VIII. CONCLUSION

In conclusion, we have performed a detailed study of the electronic and magnetic structure of $c(2\times 2)$ S chemisorbed above magnetic Fe(001). The investigation has included a first-principles determination of the height of the S [in excellent agreement with the result of LJJM (Ref. 8)], perpendicular vibrational frequency, and work function. We have found a number of important adsorption-induced changes in the Fe-like surface state spectrum, which not only have been ignored in previous ARUPS experiments but probably have bearing on the poisoning of iron's catalytic value in the Fischer-Tropsch synthesis of hydrocarbons. We have found good agreement between our calculated work-function change and sulfurlike SS's and SR's with experiment, and suggested a variety of new experiments, including electron energy-loss spectroscopy (EELS) measurements of the perpendicular vibrational frequency of the S adsorbate, spin-resolved ARUPS and KRIPES measurements of various spectral features (most notably the observation of a sulfur-induced level repulsion between $\bar{\Delta}_2$ Fe SS's near $\bar{X}_2$), as well as related UPS and IPS measurements. We have found from comparison with the earlier paramagnetic results of FW that magnetism plays a critical role in the electronic structure through the large exchange splitting of Fe and made additional predictions concerning the adsorption-induced changes in various magnetic quantities. Finally, through a detailed analysis of the DOS, band structures, plots of differences between the density before and after the adsorption, and various energy-resolved plots involving occupied and unoccupied portions of the spectrum, we have isolated the orbital character of the most important adsorption-induced changes in the spectrum and drawn a variety of conclusions concerning the relevance of our results to questions related to the sulfur-induced poisoning of an Fe catalyst.

ACKNOWLEDGMENTS

We acknowledge valuable discussions with David Singh, C. S. Wang, and Henry Krakauer and useful criticism of the manuscript by J. J. Krebs, F. A. Volkening, D. D. Johnson, and M. R. Pederson. One of us (S.R.C.) acknowledges partial support through the National Research Council and Naval Research Laboratory. Our computational support was provided by the Naval Research Laboratory though an internal grant and by the Pittsburgh Supercomputing Center.

[1]E. Wimmer, H. Krakauer, M. Weinert, and A. J. Freeman, Phys. Rev. B **24**, 864 (1981).

[2]M. Weinert, E. Wimmer, A. J. Freeman, and H. Krakauer, Phys. Rev. Lett. **47**, 705 (1981); M. Weinert, E. Wimmer, and A. J. Freeman, Phys. Rev. B **26**, 4571 (1982).

[3]S. R. Chubb and W. E. Pickett, Phys. Rev. Lett. **58**, 1248 (1987); S. R. Chubb and W. E. Pickett, Solid State Commun. **62**, 19 (1987).

[4]M. Weinert and J. W. Davenport, Phys. Rev. Lett. **54**, 1547 (1985); Cyrus Umnrigar and John W. Wilkins, *ibid.* **54**, 1551 (1985); S. R. Chubb, E. Wimmer, and A. J. Freeman, Bull. Am. Phys. Soc. **30**, 599 (1985).

[5]R. Biswas and D. R. Hamann, Phys. Rev. Lett. **56**, 2291 (1986); M. Weinert, A. J. Freeman, and S. Ohnishi, *ibid.* **56**, 2295 (1986).

[6]Kazuyuki Ueda and Ryuichi Shimizu, Jpn. J. Appl. Phys. **12**, 1869 (1973).

[7]Cf. Fig. 1 in S. R. Chubb, E. Wimmer, A. J. Freeman, J. R. Hiskes, and A. M. Karo, Phys. Rev. B **36**, 4112 (1987).

[8]K. O. Legg, F. Jona, D. W. Jepsen, and P. M. Marcus, Surf. Sci. **66**, 25 (1977).

[9]R. A. DiDio, E. W. Plummer, and W. R. Graham, Phys. Rev. Lett. **52**, 683 (1984).

[10]Gayanath W. Fernando and John W. Wilkins, Phys. Rev. B **33**, 3709 (1986).

[11]U. von Barth and L. Hedin, J. Phys. C **5**, 1629 (1972).

[12]C. S. Wang and A. J. Freeman, Phys. Rev. B **19**, 793 (1977).

[13]David Singh, Henry Krakauer, and C. S. Wang, Phys. Rev. B **34**, 8391 (1986).

[14]The explicit transformation is derived by requiring equality of the three-dimensional and two-dimensional plane-wave representations of the charge for the interstitial and vacuum regions for the case in which there is one Fe atom per layer with the corresponding representations of the charge for the case of two Fe atoms per layer at all real-space points of the associated two- or three-dimensional, two atoms per layer unit cell. Application of the plane-wave orthogonality relations for the smaller $[c(2\times 2)]$ reciprocal lattice then leads to a relationship in which the associated expansion coefficients for the $c(2\times 2)$ density are expressed as a linear combination of the comparable coefficients for the lattice involving one atom per layer.

[15]V. S. Fomenko, in *Handbook of Thermionic Properties,* edited by G. V. Samsanov (Plenum, New York, 1966).

[16]H. Kobayashi and S. Kato, Surf. Sci. **12**, 398 (1968).

[17]S. R. Chubb (unpublished). The semirelativistic sulfur atom with three majority-spin and one minority-spin p states is more tightly bound than the paramagnetic atom by more than 58 mRy.

[18]S. R. Chubb, E. Wimmer, and A. J. Freeman (unpublished).

[19]Charles W. Bauschlicher and Paul S. Bagus, Phys. Rev. Lett. **54**, 349 (1985); **52**, 200 (1984).

[20]P. J. Feibelman and D. R. Hamann, Phys. Rev. Lett. **52**, 61 (1984); Surf. Sci. **149**, 48 (1985).

[21]Alexis T. Bell, Catal. Rev. Sci. Eng. **23**, 203 (1981).

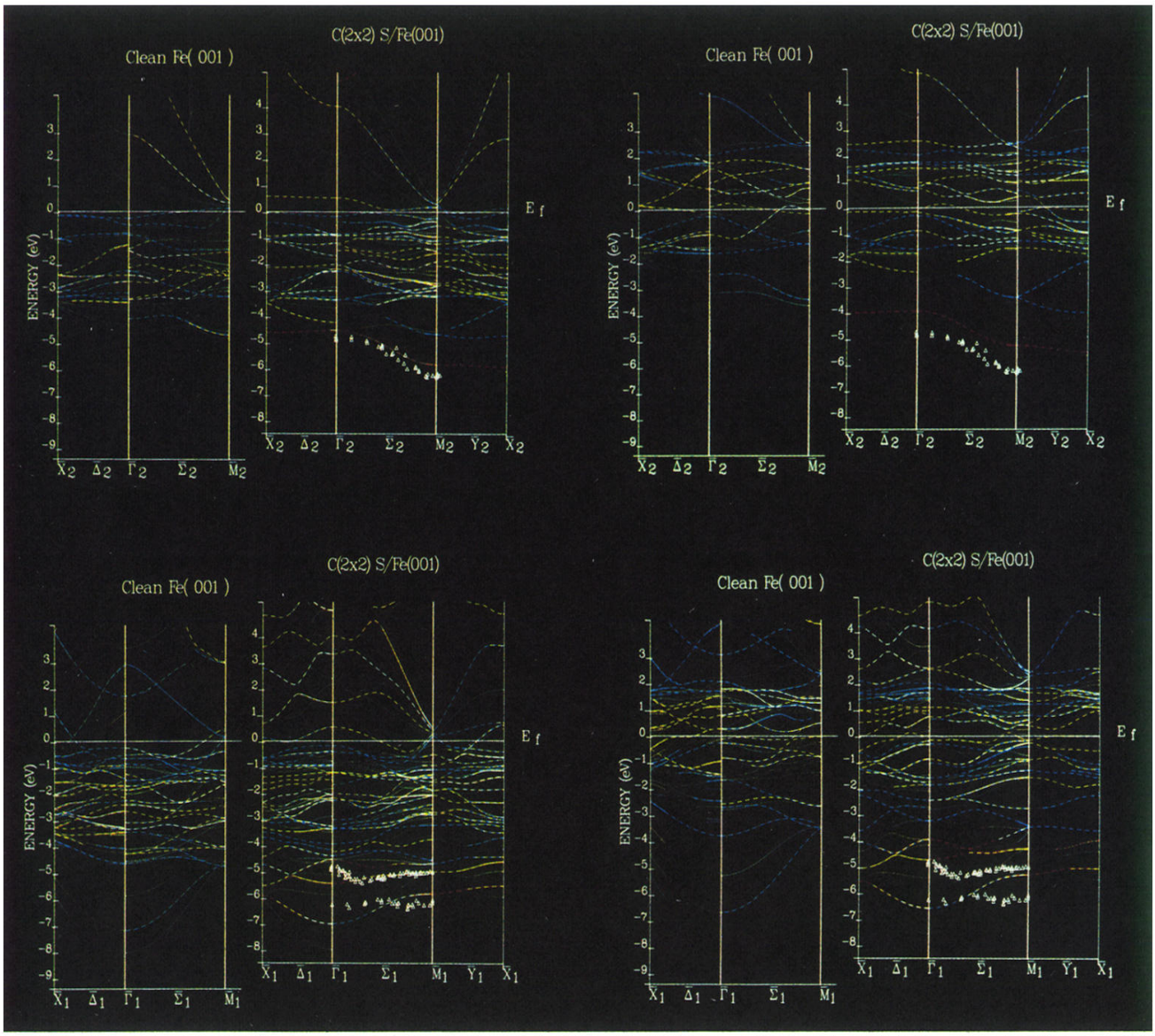

FIG. 10. The majority (left) and minority (right) band structures along the boundary of the $c(2\times2)$ SBZ, as defined in Fig. 1(b), before [clean Fe(001)] and after the adsorption; the clean Fe(001) bands are derived by folding back the spectrum for the SBZ of the single atom per layer unit cell (cf. Ref. 7). Bands are resolved by odd (even) symmetry with respect to reflection through the plane normal to the surface containing the wave vector, and denoted by the subscripts "2" ("1") beneath each point of high symmetry. Dotted (dashed) bands are even $(+)$ and odd $(-)$ with respect to z reflection through the center of the film. The coloring of bands distinguishes between states which have their largest muffin-tin charge within a particular sphere: respectively, red, yellow, green, aqua, or blue is to be associated with the S, Fe(S), Fe($S-1$), Fe($S-2$), or Fe($S-3$) sphere. Also plotted are results from non-spin-polarized angle-resolved UPS experiments by DiDio, Plummer, and Graham (Ref. 9) for the positions of sulfurlike surface states.